Enzyme-Based Hydrogels Containing Dextran as Drug Delivery Carriers: Preparation, Characterization, and Protein Release

Junying Lai,[1,2] Rui Fang,[2] Li-Qun Wang,[2] Kehua Tu,[2] Changsheng Zhao,[2] Xiaoqian Qian,[1] Shulin Zhan[1]

[1]*Department of Engineering, College of Civil Engineering and Architecture, Zhejiang University, Hangzhou 310027, China*
[2]*Institute of Polymer Science, Key Laboratory of Macromolecular Synthesis and Functionalization, Ministry of Education, Zhejiang University, Hangzhou 310027, China*

Received 22 December 2007; accepted 17 March 2009
DOI 10.1002/app.30436
Published online 27 May 2009 in Wiley InterScience (www.interscience.wiley.com).

ABSTRACT: Novel enzyme-based hydrogels for drug delivery were prepared by combining dextran with 5,5′-azodisalicylic acid using isophorone diisocyanate as the crosslinking agent. The structure of the resultant dextran/5,5′-azodisalicylic acid hydrogels was determined by infrared spectra, and the properties of the hydrogels were characterized by swelling measurements and scanning electron microscopy analysis. It was found that changing the concentration of 5,5′-azodisalicylic acid affected the crosslinking density of the hydrogels and resulted in significant differences in the water swelling property and degradability of the hydrogels. Compared with their degradability, the degradation of the hydrogels seemed to be more pronounced by azoreductase in cecum content medium than that by hydrolysis in phosphate buffer solution (PBS). Also, the release rate of the protein in cecum content medium was faster than that in PBS. Attributing to the results of the resultant hydrogels described earlier, it could be concluded that dextran/5,5′-azodisalicylic acid hydrogels could be used as a potential enzyme-based carrier for colon-specific drug delivery.
© 2009 Wiley Periodicals, Inc. J Appl Polym Sci 113: 3944–3953, 2009

Key words: hydrogels; enzyme-based; dextran; degradation; drug delivery

INTRODUCTION

Hydrogels are a class of hydrophilic, three-dimensionally crosslinked polymeric materials, which are presently used in a wide variety of applications in the medical pharmaceutical and related fields such as wound dressings, artificial organs, and drug delivery systems.[1–3] Special kinds of hydrogels, called intelligent or stimuli-responsive hydrogels, exhibit significant transitions in response to small changes of environmental conditions, simulating changes in biological systems, such as pH, ionic strength, temperature, etc.[4–9] In recent years, particular interest has been devoted to hydrogels for specific delivery of drug to the colon utilizing the intestinal microflora.[10,11] The microbial enzyme activities predominantly present in the colon that ferment these enzymes include dextranases, azoreductases, h-glucuronidase, h-xylosidase, esterases, etc.[12] These enzymes are exploited in colonic drug delivery by using them to degrade polymeric matrices. For this application, it is often required that the originally three-dimensional structure has to disintegrate preferably in harmless products to ensure a good biocompatibility of the hydrogel.

Like a number of naturally occurring polysaccharides, dextran is nontoxic, biocompatible, and stable in the upper intestine; however, they are susceptible to degradation through certain kinds of microbial enzymes, dextranase, in the colon of the human body.[13] Dextran can be chemically modified to optimize specific properties, like the ability to form hydrogel. Several approaches to prepare dextran hydrogels have been adopted. Hovgaard and Brondsted[14] obtained hydrogels directly by crosslinking dextran with 1,6-hexanediisocyanate. By polymerization of acrylate, dextran also led to the formation of the polymer network.[15]

Because azo functions can be reduced based on a special kind of microbial enzyme, azoreductase, present in the colon site, some azo aromatic compounds have been synthesized. 5,5′-Azodisalicylic acid (Olsalazine, OLZ), the biodegradability and low toxicity of azo aromatic compound, has been successfully used in clinic as an orally administrated drug. This compound is converted into therapeutically active mesalamine (5-aminosalicylic acid) component by colonic bacteria.[16,17] In addition, a number of novel polymeric

Correspondence to: K. Tu (tukh@zju.edu.cn).
Contract grant sponsor: National Nature Science Foundation of China; contract grant number: 20474055.

© 2009 Wiley Periodicals, Inc.

hydrogels containing azo groups in the crosslinks have also been synthesized.[18–21] Once inside the colon, highly swollen aromatic azo bond-containing hydrogels become accessible to azoreductase activities, which results in the reduction of the azo bond and the degradation of the hydrogel matrix.

In this study, to further promote selective degradation in the colonic environment, a novel type of enzyme-based hydrogel was constructed by combining the biocompatibility and hydrophilicity of dextran backbond with OLZ, using isophorone diisocyanate as the crosslinking agent. The preparation and properties of dextran/5,5′-azodisalicylic acid (dextran/OLZ) crosslinked hydrogels with different crosslinking density are reported in this article. The swelling properties of the resultant hydrogels in water have been determined. The dry weight changes and the morphology of the degraded hydrogels by azoreductase in rat cecum contents and by hydrolysis in phosphate buffer solution (PBS) have been investigated. The drug release behaviors of hydrogels are also determined by choosing bovine serum albumin (BSA) as the model drug.

EXPERIMENTAL

Materials

5,5′-Azodisalicylic acid was purchased from Zhongyi Pharmaceutical (Jinhua, China). Dextran (M_n: 40,000), α-D-glucose, dicyclohexyl carbodiimide (DCC), *N*,*N*′-dimethyl amino pyridine (DMAP), isophorone diisocyanate (IPDI), and BSA were purchased from Acros (Geel, Belgium). Benzyl viololgen (BV) was purchased from Aldrich (St. Louis, MO). DMAP was recrystallized from distilled ethyl acetate and stored over silica gel at 0°C. DCC was distilled under diminished pressure (bp 130°C/3 mmHg). Tetrahydrofuran (THF) was dried with CaH_2 and distilled. Dimethyl sulfoxide (DMSO) was distilled under decompression. The other chemicals were used as received.

Characterizations

Infrared (IR) spectra were recorded with a Bruker Vector 22 Fourier transform infrared instrument. ^{1}H- and ^{13}C-NMR spectra were obtained with an Avance DMX 500-MHz spectrometer using DMSO-d_6 as a solvent. Ultraviolet–visible (UV–vis) spectra were carried on a Cary 100 Bio UV–vis spectrophotometer. Scanning electron microscope (SEM) images were taken on a Philips XL-30ESEM.

Preparation of di(2-hydroxyethyl) 5,5′-azodisalicylate

Di(2-hydroxyethyl) 5,5′-azodisalicylate was synthesized following the procedures of our previous work,[22] i.e., OLZ was esterified by ethylene glycol with DCC as coupling agent and DMAP as basic catalyst. Briefly, OLZ (6 g, 20 mmol) and ethylene glycol (4 g, in excess) were dissolved in 40 mL of THF in a sealed flask at room temperature. After nitrogen being purged for 30 min, DMAP (0.7 g, 6 mmol) and DCC (10.3 g, 50 mmol) in 10 mL of THF were added successively. The reaction was continued for 24 h at room temperature with stirring and nitrogen atmosphere protection. At the completion of reaction, the product was purified by precipitation method and dried under vacuum (yield 73%). The dried product was characterized by FTIR, ^{1}H-NMR, and ^{13}C-NMR.

Preparation of dextran/OLZ hydrogels

With stannous caprylate as catalyst, di(2-hydroxyethyl) 5,5′-azodisalicylate was dissolved in DMSO and then added to the solution of twofold molar IPDI. After being stirred for half an hour at room temperature under dried nitrogen, the reaction mixture was added into the dextran solutions (DMSO as solvent) under dried nitrogen. The feed compositions and sample identification of the reactions are listed in Table I. The mixtures were then diverted into glass mold and reacted at 70°C for 24 h. The products were dialyzed in deionized water, which was refreshed every 4 h to remove the reagent residues until the absorbance of the surrounding solvent of the gels was no longer detectable by UV–vis spectra (200 nm $< \lambda <$ 600 nm). The dextran/OLZ crosslinked hydrogels were then carefully cut into small disks (about 15 mm in diameter and 3 mm in

TABLE I
The Composition of Dextran/OLZ Hydrogels

Sample ID	Feed composition				Azo bond content measured[a] (mmol)	Crosslinking density (mol %)	Yield (%)
	Di(2-hydroxyethyl) 5,5′-azodisalicylate (mmol)	IPDI (mmol)	Hydroxyl group of dextran (mmol)	DMSO (mL)			
Gel-1	0.125	0.25	8	8	0.028	0.7	76.1
Gel-2	0.25	0.50	8	8	0.056	1.4	80.8
Gel-3	0.375	0.75	8	8	0.144	3.6	78.4
Gel-4	0.5	1	8	8	0.288	7.2	83.0

[a] The content of azo bonds were determined spectrometrically.

thickness) and dried to constant weight under vacuum. Then, these dried hydrogel disks were used in the following measurements, such as swelling, SEM, degradation, and BSA release. The yields of the hydrogels are listed in Table I. The hydrogel products were characterized by FTIR.

Determination of the content of aromatic azo bonds in the hydrogels

The amount of aromatic azo bonds in the hydrogels was determined spectrophotometrically.[19] Briefly, dried hydrogel samples (about 50 mg) were weighted and suspended in NaOH (2 mol/L, 20 mL). The suspension was incubated at 37°C for 3 days to dissolve the hydrogel. The resulting solution was diluted 10 times with deionized water. Then the content of azo bonds in hydrogels was determined at 365 nm using UV–vis spectrophotometer.

The crosslinking density of dextran/OLZ hydrogels is defined as follows:

$$\text{Crosslinking density (\%)} = [\text{Azo bond content (molar)} \times 2 / \text{Hydroxyl group of dextran (molar)}] \times 100.$$

Swelling experiments of dextran/OLZ hydrogels

The sorption capacity of dextran hydrogels was determined by swelling the dried hydrogel disks in deionized water at 37°C. The hydrogels were removed from the water bath at regular time intervals and blotted with filter paper to remove excess water on the surface and weighed. Afterward, they were returned into the same swelling bath until equilibrium was attained. The average value of three measurements was taken for each sample. The swelling ratio can be calculated using the following equation:

$$\text{Swelling ratio (\%)} = [(W_s - W_d)/W_d] \times 100, \quad (2)$$

where W_s and W_d are the weight of the swollen and dry state of the sample, respectively.

Morphology of dextran/OLZ hydrogels

The dried hydrogel disks were first equilibrated in deionized water at room temperature, quickly frozen in liquid nitrogen thereafter, and further freeze-dried in a freeze drier under vacuum at –42°C for at least 3 days until all the solvent was sublimed. The freeze-dried hydrogel was then fractured carefully and the interior morphology of the hydrogel was studied using SEM. Before SEM observations, specimens of the hydrogel were fixed on aluminum stubs and coated with gold for 240 s.

The degradation properties of dextran/OLZ hydrogels

The degradation of the resultant hydrogels by hydrolysis was carried out in PBS. The hydrolysis of dextran/OLZ hydrogels were performed in 0.1*M* PBS of pH 7.4 at 37°C. At chosen time intervals, the hydrogel disk was retrieved and washed cleanly with deionized water. Later, the gel was dried under vacuum. Changes in the dried weight of the hydrogels were determined to evaluate the degradation process.

In addition, the biodegradation of the hydrogels by azoreductase was carried out in the rat whole-cell cecum content extract. Such an extract was isolated by a procedure described in Refs. 23–25. Then, 10 mL of cell suspension (1.0 g fresh weight cecum content/25 mL, containing α-D-glucose, 14 h preincubation) was mixed with 1 mL of 1 m*M* BV or distilled H_2O. The final concentration of the enzyme-containing solution is as follows: 0.025 g/mL of rat cecum content, 62.5 μ*M* BV, and 1.25 mg/mL α-D-glucose. The hydrogels immersed in rat cecum content medium (RCCM) was incubated under anaerobic condition at 37°C in a shaking chamber. At chosen time intervals, the hydrogel disk was retrieved and washed cleanly with deionized water. Later, the gel was dried under vacuum. The changes of the dried weight of the hydrogels were determined to evaluate the degradation process.

The interior morphology of the degrading samples was observed by SEM with freeze-dried manipulation after washing cleanly with deionized water.

BSA incorporation and release of dextran/OLZ hydrogels

BSA was chosen as the model compound for large macromolecular protein-based drugs. BSA loading solution was prepared by first dissolving 4 g BSA in 200 mL of distilled water. BSA was loaded into the dried hydrogel disks via equilibrium partition in a BSA solution as prepared earlier, i.e., by placing the dried dextran/OLZ hydrogel disks into BSA solution at 37°C for 1 day. Thus, BSA was loaded into each hydrogel disk up to equilibrium by swelling in the BSA-containing solution. For the confirmation of percentage of drug loading in hydrogels, the amount of BSA solution left in the loading medium was determined by measuring the optical density at 280 nm using UV–vis spectrophotometer. The total BSA uptake in the hydrogles can be calculated using the following equation:

$$\text{The total BSA uptake} = (W_0 - W_1)/W_2, \quad (3)$$

where W_0, W_1, and W_2 denote the weight of overall BSA in solution, the weight of left BSA in solution, and the weight of the dried hydrogel disk used, respectively.

For the drug release kinetic studies *in vitro*, the drug-loaded hydrogels were immersed in 25 mL PBS and RCCM under anaerobic condition, respectively, and were left in a shaking water bath at 37°C. Samples were withdrawn at regular intervals, and the release of BSA was estimated using UV spectrophotometer. With each sampling, the solution was returned into the same bath under anaerobic condition.

RESULTS AND DISCUSSION

Preparation of dextran/OLZ hydrogels

Figure 1 shows the schematic of the chemical reactions. The structure of di(2-hydroxyethyl) 5,5′-azodisalicylate was confirmed by ^{1}H-NMR (Fig. 2) and ^{13}C-NMR (Fig. 3). In the ^{1}H-NMR spectrum, the peaks at 7.1–8.4 ppm belong to the phenyl group, and the peaks 3.77 and 4.39 ppm are characteristic of the methylene units. The resonance of the aliphatic hydroxyl group is observed at 5.25 ppm, and the resonance of the phenolic hydroxyl group is observed at 10.95 ppm. In the ^{13}C-NMR spectrum, the carbons of benzene appear at 114–163 ppm and

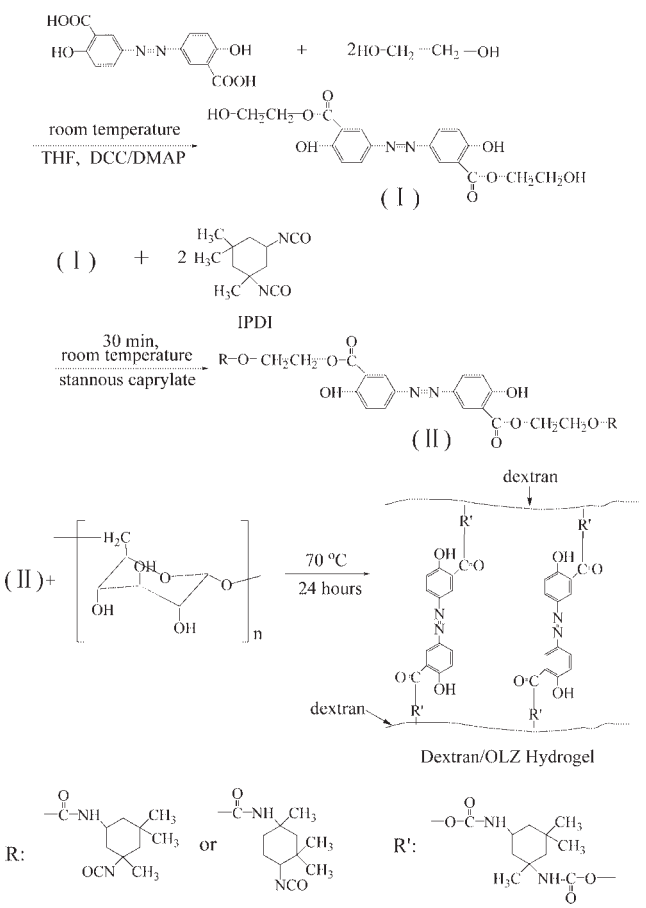

Figure 1 The chemical structure of dextran/OLZ hydrogel.

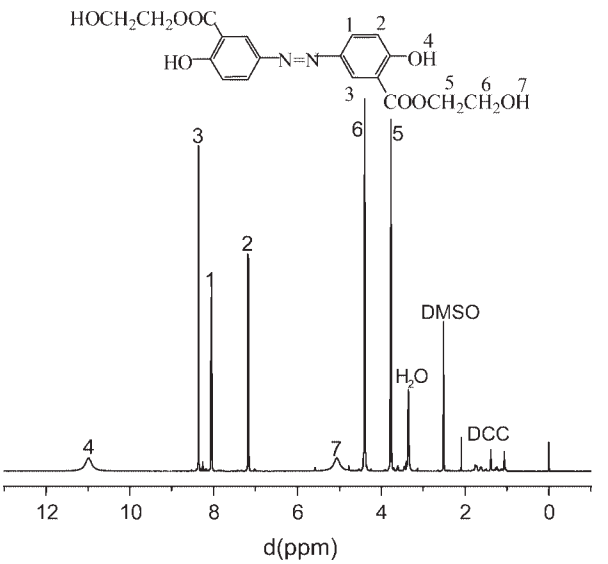

Figure 2 ^{1}H-NMR spectra of di(2-hydroxyethyl) 5,5′-azodisalicylate.

the peaks 57.3 and 67.8 ppm belong to the carbons of methylene units. The peak at 168.6 ppm is characteristic of carboxylate carbon.

Using IPDI as crosslinking agent, dextran/OLZ hydrogels were prepared. The products were purified in deionized water to remove the reagent residues until the absorbance of the surrounding solvent of the hydrogels was no longer detectable by UV–vis spectra. The structure of the hydrogels was analyzed by FTIR (Fig. 4). The IR spectrum shows characteristic bands at 3360 cm^{-1} corresponding to the stretching vibration of N—H and O—H. The characteristic C=O out of bending vibration of urethane appears at 1730 cm^{-1}. The C—O stretching vibrations of ether appear at 1020 cm^{-1}. By adjusting the feed compositions, the crosslinking densities of the hydrogels

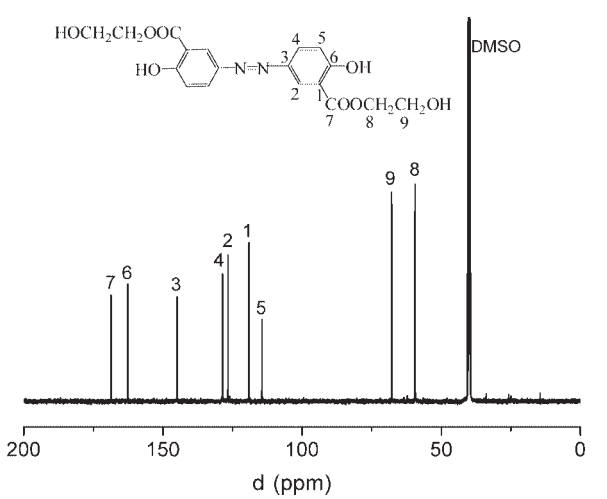

Figure 3 ^{13}C-NMR spectra of di(2-hydroxyethyl) 5,5′-azodisalicylate.

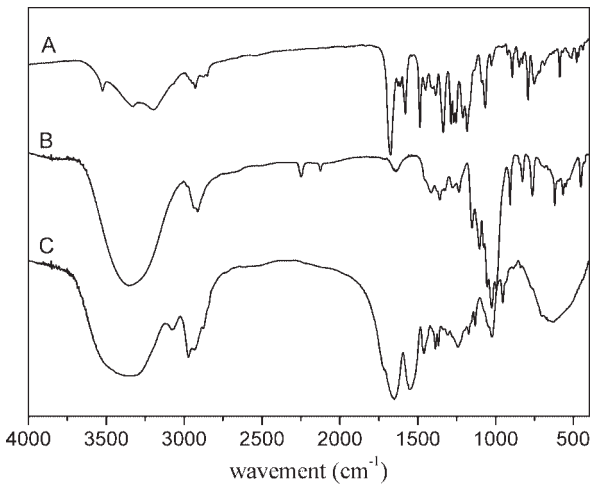

Figure 4 FTIR spectra of di(2-hydroxyethyl) 5,5′-azodisalicylate (A), dextran (B), and dextran/OLZ hydrogel (C).

were varied from 0.7 to 7.2%, calculated as molar of azo bond content of the hydrogel in percent of molar of hydroxyl group of dextran (summarized in Table I). The azo bonds content of the hydrogels is less than the feed di(2-hydroxyethyl) 5,5′-azodisalicylate. This may be the reason why di(2-hydroxyethyl) 5,5′-azodisalicylate reacts incompletely with IPDI, and the remaining di(2-hydroxyethyl) 5,5′-azodisalicylate cannot react with dextran. So, the measured crosslink densities are less than the prediction. The excessive IPDI would react directly with dextran.

Water swelling property

Soluble polymers and crosslinkers were extracted before the equilibrated study. The water uptake of initially dried hydrogels was followed for a period of time, gravimetrically. Swelling curves of the hydrogels are constructed and shown in Figure 5 where the swelling increases with time up to a certain level and then levels off. It is observed that hydrogels with the crosslinking density of 0.7 mol % (relative to hydroxyl group concentration of dextran) presents equilibrium swelling ratios of about 745%. When the crosslinking density increased to 7.2 mol % (Gel-4), the equilibrium swelling ratios decreased to 136%. It is well known that hydrogel swelling is limited by crosslinking density. If the crosslinking density is greatly increased, the hydrogels present a tighter structure, which decreases the average pore size, and the water-absorption capability of the hydrogels decreases significantly. Figure 5 also shows that the swelling ratios of Gel-3 and Gel-4 are close (166% for Gel-3, and 136% for Gel-4). This could be attributed to the side reaction that the excessive IPDI reacts with dextran directly. Also, it would increase the actual crosslink density of hydrogels.

Interior morphology of dextran hydrogels

The interior morphology of dextran/OLZ hydrogels under swollen condition is shown in Figure 6. Swollen dextran/OLZ hydrogels were frozen in liquid nitrogen and then freeze-dried before SEM morphological investigation. Although this treatment may lead to structural artifacts of the specimens, the SEM photographs clearly show that the morphology of dextran/OLZ hydrogel exhibits a homogeneous porous architecture. Moreover, the differences in morphology observed among the resultant hydrogels are presumably of intrinsic nature because the fixation procedures were identical among all dextran/OLZ hydrogels. The most distinctive feature in Figure 6 is that dextran/OLZ hydrogels exhibit different diameters of porous, which presumably result from the differences in crosslinking density in network moiety. The morphological characteristics of the hydrogels tend to decrease the diameter of pores with increased crosslinking density. The results are in agreement with the changes seen in the swelling properties.

Based on the swelling property and SEM morphology observed, these dextran/OLZ hydrogels are expected to have different degradability and drug release properties by controlling the crosslinking density of hydrogels. The degradability and drug release data, as described later, are also significantly affected by this crosslinking structure.

Degradability of dextran/OLZ hydrogels

Dextran/OLZ hydrogels are based on degradable polysaccharide backbond combined with a redox-sensitive aromatic azo function. In our previous research,[22] the degradability of linear PEO-OLZ copolymer in RCCM and PBS, respectively, was observed. The results show that azo bond is

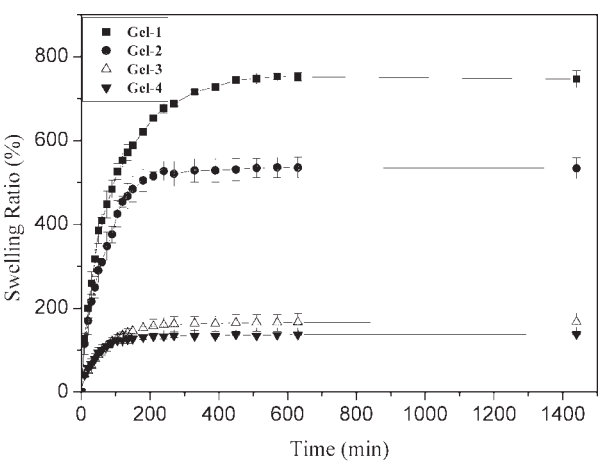

Figure 5 Time-dependent swelling ratio of dextran/OLZ hydrogels in deionized water at 37°C ($n = 3$).

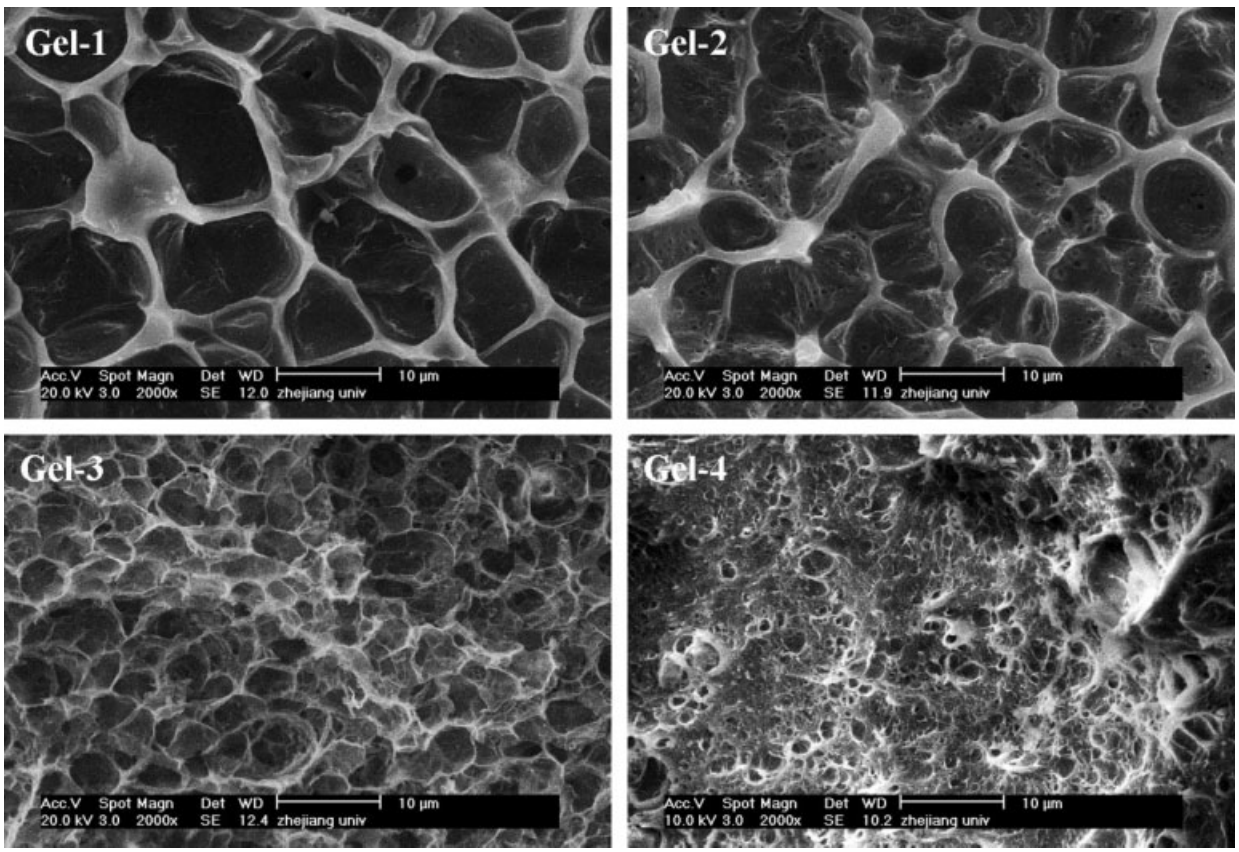

Figure 6 SEM micrographs of swollen hydrogels in deionized water at 37°C for 1 day.

susceptible to degradation through a special kind of microbial enzyme, azoreductase, in the colon site of the human body. In addition, the ester bonds in di(2-hydroxyethyl) 5,5′-azodisalicylate segments can be hydrolyzed in PBS. The degradation rate of the hydrogels is faster in RCCM than in PBS. In this study, the degradability of the hydrogels by azoreductase was carried out primarily in rat whole-cell cecum contents medium. The degradation experiment of ester bonds in PBS was also observed.

As mentioned earlier, dextran/OLZ hydrogels can be degraded in PBS and RCCM. The weight changes of the dry hydrogels in PBS and RCCM are shown in Figures 7 and 8, respectively. The dry weight of the hydrogels decreased during the degradation process. However, the magnitudes of the decrease were largely dependent on the crosslinking density (aromatic azo content) of the hydrogel. The lower the aromatic azo content in the gel, the faster is the loss of dry weight. The degradation rate of the same

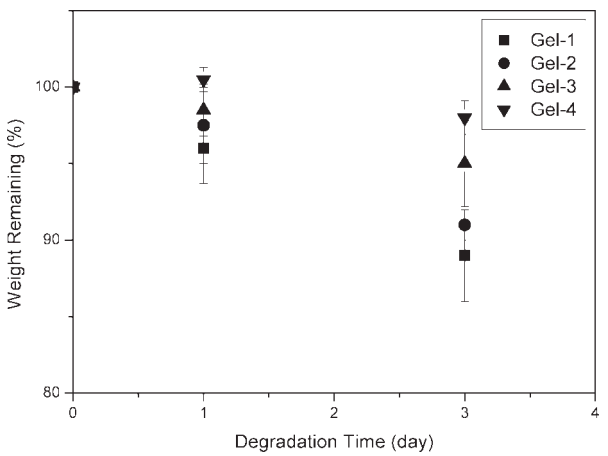

Figure 7 The changes of dry weight of dextran/OLZ hydrogels in PBS ($n = 3$).

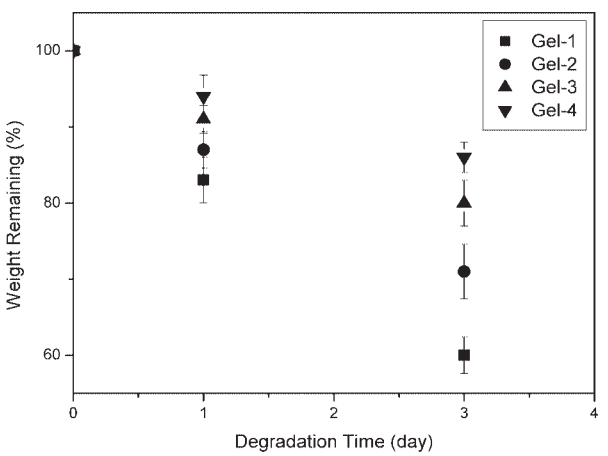

Figure 8 The changes of dry weight of dextran/OLZ hydrogels in rat cecum content medium ($n = 3$).

hydrogel sample should change in different degradation mediums. For example, it is less than 12% weight loss of Gel-1 incubated in PBS for 3 days. However, it is more than 17% and 28% weight loss of Gel-1 incubated in RCCM for 1 day and 3 days, respectively. The other dextran/OLZ hydrogel samples have the similar rule when degraded in PBS and RCCM. The hydrogels are degraded in PBS because of the hydrolysis of the ester bonds in the network. In RCCM, the hydrogels are degraded mainly because of the reduction of azo bonds. It might be concluded that the degradation rate of dextran/OLZ hydrogels is much faster in the biological medium with rat cecum contents than that in PBS.

Visual examinations of the degraded hydrogel samples were carried out using SEM to observe changes of the structure of the gel. The micrographs are shown in Figures 9–11 for the hydrogels at degradation time of 3 days in PBS and 1 day and 3 days in RCCM, respectively.

Figure 9 presents the interior morphology of the degraded hydrogels after incubation in PBS at 37°C for 3 days. It can be clearly seen from the figures that the lyophilized hydrogel membrane appears to be compact and the pores size of the samples become larger than the swollen samples in deionized water for 24 h. It is because the ester linkage in the hydrogels has tendency to undergo hydrolysis, and the prepared dextran/OLZ hydrogels can degrade into dextran segments and OLZ segments when subjected into PBS environment. However, the degree of hydrolysis in the hydrogels samples is relatively feeble. It may be the three-dimensional structure preventing the further dissolution of the hydrogels, so the hydrolysis of ester bonds becomes difficult.

To evaluate the enzyme degradation of azo bonds in dextran/OLZ hydrogels by azoreductase, the hydrogel samples were incubated in the whole-cell bacterial extract isolated from rat cecum under anaerobic condition at 37°C in a shaking chamber. If degradation occurs, it should result in a change in the interior morphology attributed to the decrease of the number of crosslink bonds by azo reduction.

As Figures 10 and 11 represent, after incubated in cecum content extracts for 1 day and 3 days, respectively, the interior morphology of dextran/OLZ hydrogels has changed significantly. It shows clearly that the degraded hydrogel networks with different crosslinking densities follow the same trend when the incubation time is prolonged. That is, structural deterioration of the hydrogels is observed and pores developed on the membranes, and the broken pores are clearly found on the edges of some hydrogels. However, there are some morphological differences

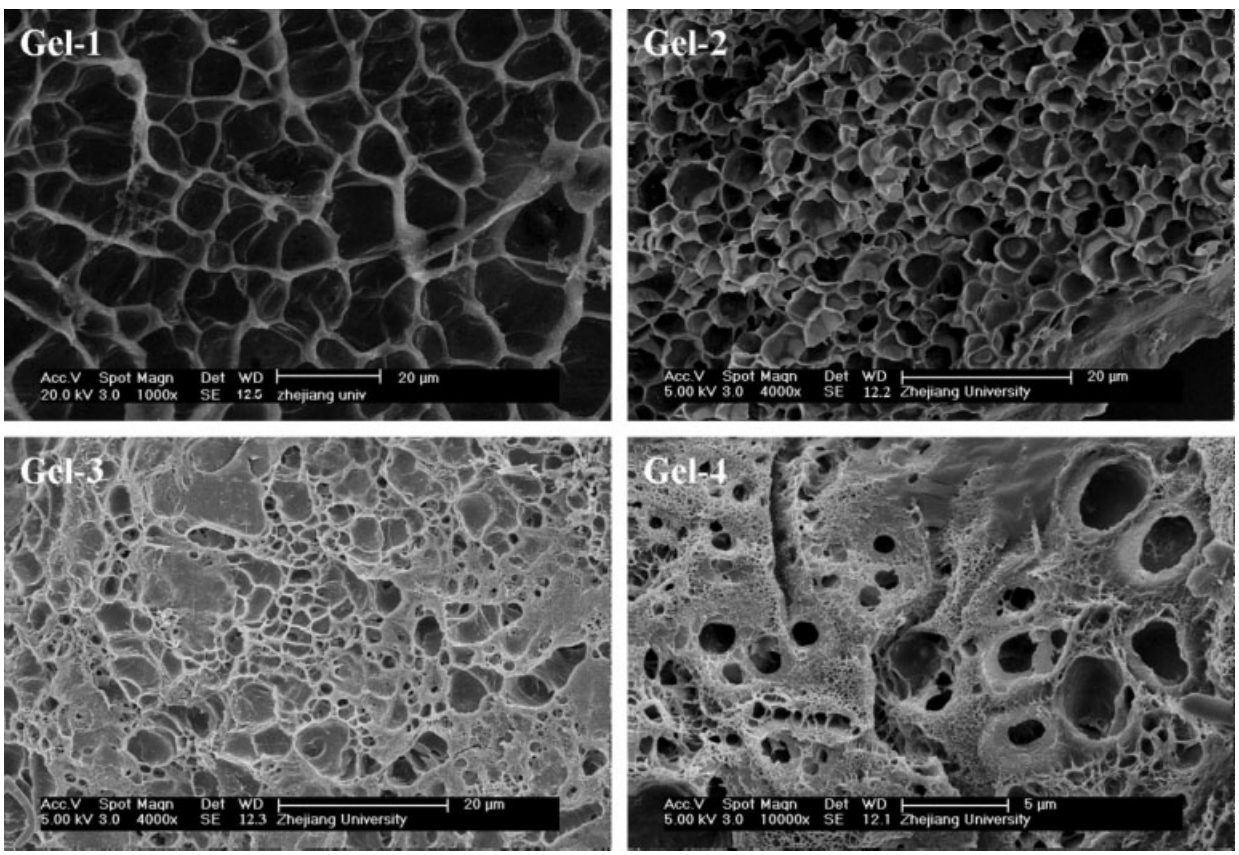

Figure 9 SEM micrographs of degraded hydrogels incubated in PBS under anaerobic condition at 37°C for 3 days.

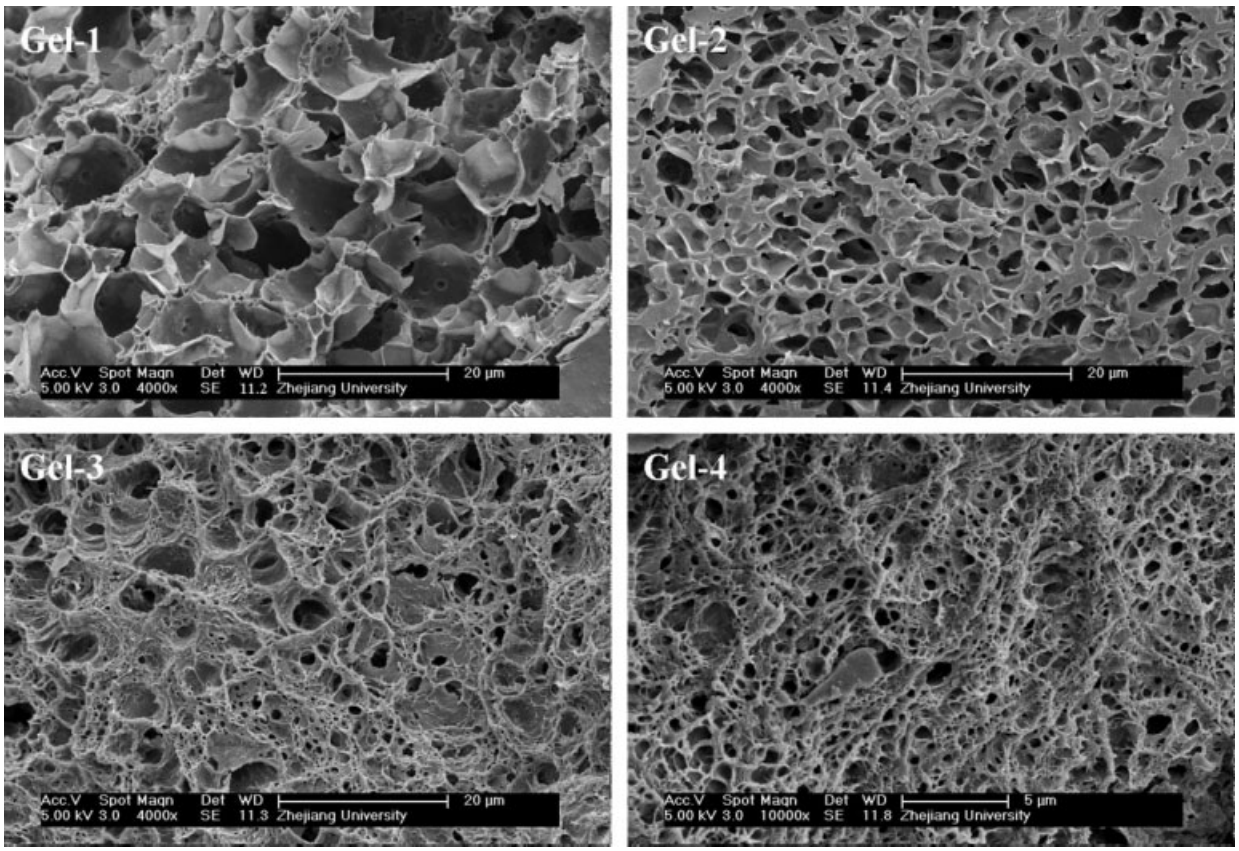

Figure 10 SEM micrographs of degraded hydrogels incubated in rat cecum contents medium under anaerobic condition at 37°C for 1 day.

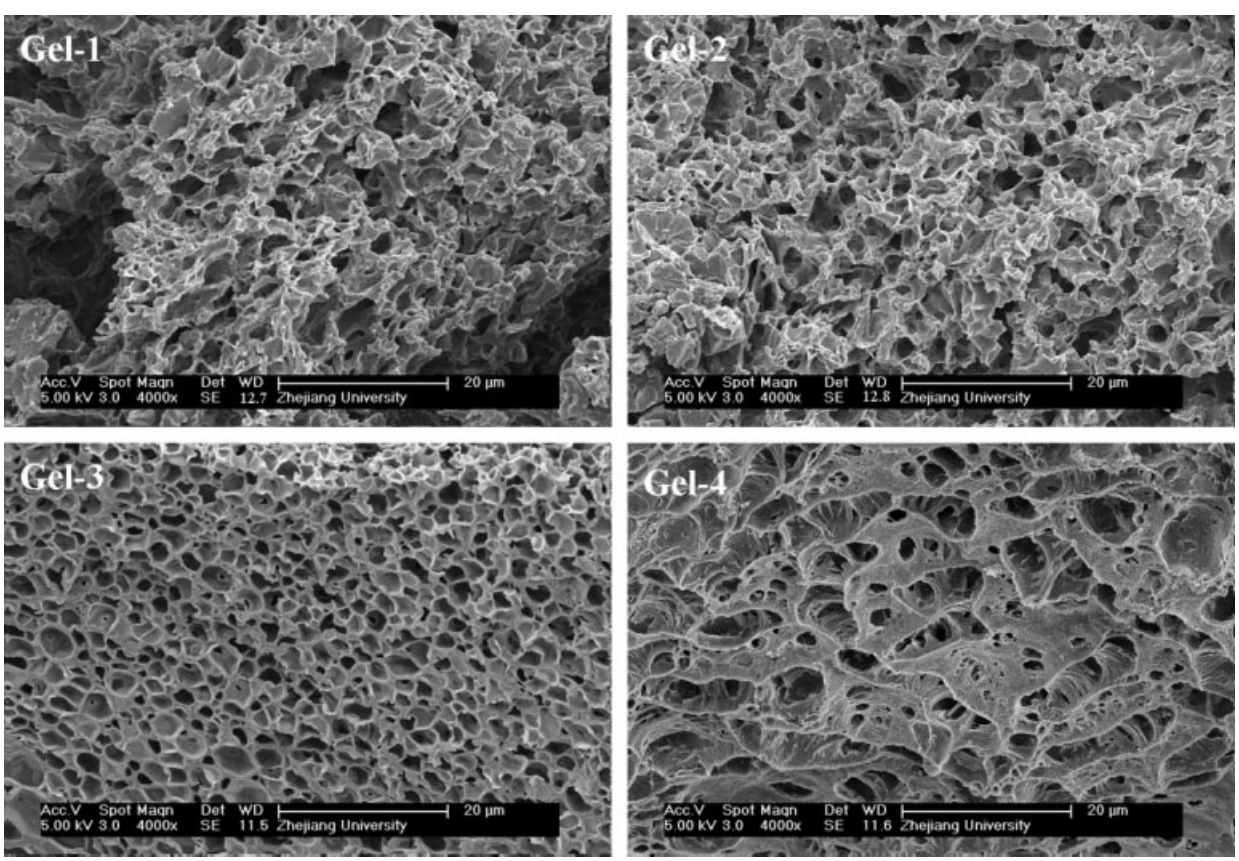

Figure 11 SEM micrographs of degraded hydrogels incubated in rat cecum content medium under anaerobic condition at 37°C for 3 days.

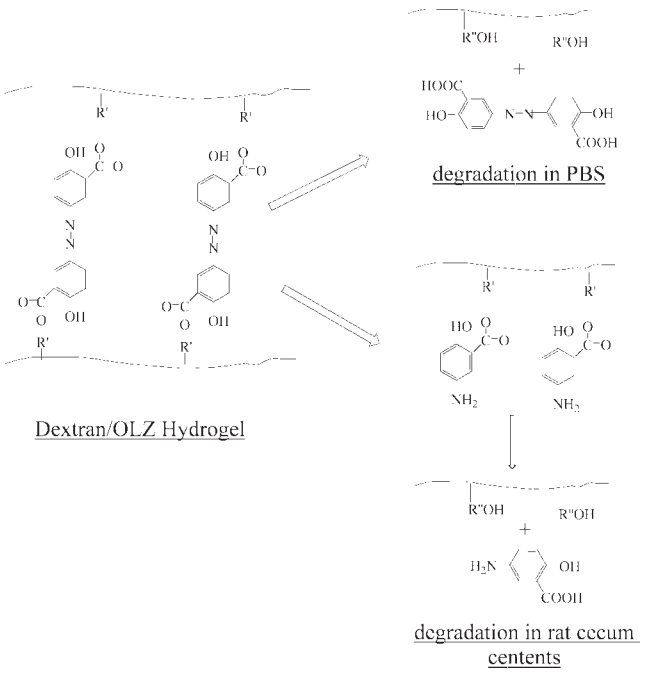

Figure 12 The biological degradation of dextran/OLZ hydrogels in rat cecum contents medium and PBS, respectively.

in these hydrogel samples. On the contrary to looser and irregular appearance of Gel-1 network, the interior structure of Gel-4 network looks far more regular and tight and seems to be compact for 1 day. After the hydrogel swelling, azoreductase diffused into polymer and the azo bonds degraded by azoreductase in cecum content medium. Increasing the crosslinking density results in a denser network; this obstructs azoreductase diffusing into the hydrogels. So, the degradation rate of Gel-4 is slower than Gel-1.

After incubating in RCCM for 3 days, a majority of pores in Gel-1 and Gel-2 are broken (Fig. 8). Based on these SEM images, the degradation rate of dextran/OLZ hydrogels is much faster in the biological medium with rat cecum contents than that in PBS, suggesting that the enzyme reaction of azo bonds should take place before the hydrolysis of the ester linkage (as shown in Fig. 12).

Protein incorporation and release from dextran/OLZ hydrogels

Drug incorporation experiments were performed by immersing dry dextran/OLZ hydrogels into BSA solutions. One day later, the swollen hydrogels were reweighed and the concentrations of BSA left in the loading medium were determined by measuring the optical density at 280 nm using UV–vis spectrophotometer. As listed in Table II, the total BSA uptake for hydrogels was dependent on the characteristics of the hydrogels and it was the lowest for Gel-4. This feature can be assigned to the fact that Gel-4 was less swollen and thus less inclined to protein incorporation. On the other hand, the drug loading capacity of dextran/OLZ hydrogel increases with its decreasing crosslinking density.

The release of BSA from dextran/OLZ hydrogels were performed by immersing the BSA-incorporated hydrogels in PBS and cecum content medium, respectively. Figure 13 depicts the release profiles of BSA from dextran/OLZ hydrogels. All of the prepared hydrogels show an initial burst release within the first 15 min with the amount of 15–35%. The possible explanation of sudden release is due to the BSA absorbed at the gel surface. Because the concentration gradient is the driving force for drug diffusion, high BSA concentration gradient between the hydrogel surface and the release medium during the very early stage of contact leads to a higher initial burst and faster release. Although the hydrogels exhibit similar release profiles, their release rates and extents are different. The release rate is found to be dependent on the crosslinking density and the presence of RCCM. The total release amount decreases with the increasing crosslinking density. When no RCCM is present in PBS, less than 50% of loading-BSA is released after 3 h. However, if RCCM is present, the release profile is faster, where the release of BSA is about 70% of loading-BSA after 3 h. The azo groups will undergo degradation by the azoreductase resulting in the faster and enhanced release of drug entrapped in RCCM than that in PBS.

TABLE II
The Total BSA Uptake and Equilibrium Release Data from Dextran/OLZ Hydrogels Incubated in PBS and Rat Cecum Content Medium, respectively, Under Anaerobic Condition at 37°C

Sample ID	Total uptake (mg/g dry gel)	Amount of the nonreleased drug (mg/g dry gel)		% Release	
		In PBS	In cecum content medium	In PBS	In cecum content medium
Gel-1	153	20	2	87.0	99.2
Gel-2	124	19	14	84.8	89.0
Gel-3	93	22	12	76.7	87.0
Gel-4	86	25	28	71.8	67.9

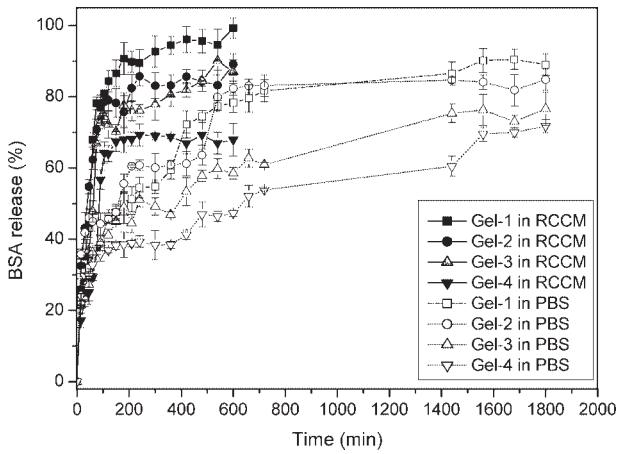

Figure 13 Release percent of BSA from dextran/OLZ hydrogel incubated in PBS and rat cecum content medium (RCCM), respectively, under anaerobic condition at 37°C ($n = 3$).

After the hydrogel swelling, azoreductase diffuses into polymer and the azo bonds degraded in cecum content medium, following a fast release rate of BSA. In contrast to what is observed in cecum content medium, the release rate of BSA in the PBS is slower relatively with the formation of a shoulder. The reason is probably that after the hydrogel swelling, the diffusion-controlled kinetics becomes weaker, and the release of BSA is chemically controlled.[2] Because the hydrolysis of the ester bonds of the hydrogels is slower than the reduction of azo bonds,[22] the release rate slows down. With the incubation time prolonging, the degradation degree of the hydrolysis of the ester linkage increases in PBS, this causes loosening of the hydrogels resulting in the release rate of entrapped drug becoming fast again. This phenomenon is more distinct in the hydrogel with high crosslinking density. However, the release rate of BSA is faster in the cecum contents than that in PBS, which insures that the protein would be of specific release in the colon. The residual BSA may be greatly entrapped within the collapsed matrix and hence retard BSA release at a longer period. The lack of BSA release after about 30 h might be attributed to the interactions between BSA and the hydrogel network, which entraps and prevents the remaining BSA from releasing.

CONCLUSIONS

In this work, novel enzyme-based hydrogels were prepared. By introducing OLZ segment with different contents to the hydrogels, the crosslinking density of the hydrogels can be adjusted readily from 0.7 to 7.2%. When the crosslinking density increased, the water-absorption capability of the hydrogels decreases significantly. Also, the process of hydrogel degradation was largely dependent on the crosslinking density of the hydrogels. The changes in dry weight and the interior morphology of the hydrogels after 3 days of degradation show that azoreductase has a more profound effect on the biodegradability of all the resultant hydrogels than PBS buffers. The release rate of the protein of BSA is faster in the cecum contents than that in PBS, which insures that drugs would be of specific release in the colon. The results suggest that dextran/OLZ hydrogels are very good candidates as enzyme-based carriers for colon-specific drug delivery.

References

1. Hennink, W. E.; van Nostrum, C. F. Adv Drug Delivery Rev 2002, 54, 13.
2. Lin, C. C.; Metters, A. T. Adv Drug Delivery Rev 2006, 58, 1379.
3. Qiu, Y.; Park, K. Adv Drug Delivery Rev 2001, 53, 321.
4. Chen, L.; Dong, J.; Ding, Y.; Han, W. J Appl Polym Sci 2005, 96, 2435.
5. Chen, L.; Tian, Z.; Du, Y. Biomaterials 2004, 25, 3725.
6. Turan, E.; Caykara, T. J Appl Polym Sci 2007, 106, 2000.
7. Zhang, X. Z.; Wu, D. Q.; Chu, C. C. Biomaterials 2004, 25, 3793.
8. Emik, S.; Gurdag, G. J Appl Polym Sci 2006, 100, 428.
9. Zhang, R.; Tang, M.; Bowyer, A.; Eisenthal, R.; Hubble, J. Biomaterials 2005, 26, 4677.
10. Maris, B.; Verheyden, L.; Reeth, K. V.; Samyn, C.; Augustijns, P.; Kinget, R.; Van den Mooter, G. Int J Pharm 2001, 213, 143.
11. Stubbe, B.; Maris, B.; Van den Mooter, G.; De Smedta, S. C.; Demeester, J. J Controlled Release 2001, 75, 103.
12. Sinha, V. R.; Kumria, R. Eur J Pharm Sci 2003, 18, 3.
13. Sinha, V. R.; Kumria, R. Int J Pharm 2001, 224, 19.
14. Hovgaard, L.; Brondsted, H. J Controlled Release 1995, 36, 159.
15. Kim, S. H.; Chu, C. C. J Biomed Mater Res 2000, 49, 517.
16. Wadworth, A. N.; Fitton, A. Drugs 1991, 41, 647.
17. Segars, L. W.; Gales, B. J. Clin Pharm 1992, 11, 514.
18. Chivukula, P.; Dusek, K.; Wang, D.; Duskova-Smrckova, M.; Kopeckova, P.; Kopecek, J. Biomaterials 2006, 27, 1140.
19. Wang, D.; Dusek, K.; Kepeckova, P.; Duskova-Smrckova, M.; Kopecek, J. Macromolecules 2002, 35, 7791.
20. Ghandehari, H.; Kepeckova, P.; Kopecek, J. Biomaterials 1997, 18, 861.
21. Shantha, K. L.; Ravichandran, P.; Panduranga, R. K. Biomaterials 1995, 16, 1313.
22. Lai, J.; Wang, L. Q.; Tu, K.; Zhao, C.; Sun, W. Macromol Rapid Commun 2005, 26, 1572.
23. Brown, J. P.; Mcgarraugh, G. V.; Parkinson, T. M., Jr.; Wingard, R. E.; Onderdonk, A. B. J Med Chem 1983, 26, 1300.
24. Kopecekova, P.; Kopecek, J. Makromol Chem 1990, 191, 2037.
25. Kopecekova, P.; Rathi, R.; Takada, S.; Rihova, B.; Berenson, M. M.; Kopecek, J. J Controlled Release 1994, 28, 211.